Bioelectrochemistry 84 (2012) 25–31

Contents lists available at SciVerse ScienceDirect

Bioelectrochemistry

journal homepage: www.elsevier.com/locate/bioelechem

Direct electrochemistry of dopamine on gold—*Agaricus bisporus laccase enzyme* electrode: Characterization and quantitative detection

Reza Karimi Shervedani *, Akbar Amini

Department of Chemistry, University of Isfahan, Isfahan 81746-73441, I.R. Iran

ARTICLE INFO

Article history:
Received 1 August 2011
Received in revised form 21 September 2011
Accepted 24 October 2011
Available online 9 November 2011

Keywords:
Laccase enzyme from *Agaricus bisporus*
Immobilization
Direct electron transfer
Dopamine
Human blood plasma

ABSTRACT

Direct electrochemistry of a new laccase enzyme immobilized on gold and its application as a biosensor for dopamine (DA) are investigated by voltammetry and electrochemical impedance spectroscopy. The sensor demonstrated a redox adsorption behavior with $E^{0'} = +180$ mV vs. Ag/AgCl for immobilized *Agaricus bisporus laccase (LacAB) enzyme*. The MPA platform was assembled on Au *with* and *without* utilization of ultrasounds. Excellent results were obtained by using the enzyme electrode fabricated based on MPA assembled *with* sonication. The *LacAB* immobilized in this condition showed a large electrocatalytic activity for oxidation of DA. Accordingly, a third-generation (mediator free) biosensor was constructed for DA. The DA concentration could be measured in the linear range of 0.5 to 13.0 and 47.0 to 430.0 μmol L^{-1} with correlation coefficients of 0.999 and 0.989, respectively, and a detection limit of 29.0 nmol L^{-1}. The biosensor was successfully tested for determination of DA in human blood plasma and pharmaceutical samples.

© 2011 Elsevier B.V. All rights reserved.

1. Introduction

Several researches have been performed to evaluate possible applications of enzymes for environmental and biotechnological intentions [1]. The oxidoreductase enzymes, either dissolved in electrolyte solutions or immobilized on solid surfaces, can serve as redox centers and react selectively with biological species. However, operational conditions for enzymatic processes in solution phase are not often suitable [2], which in turn is due to enzyme denaturation, difficulties in enzyme recovery from substrate and products, and low efficiency [3]. These problems can be successfully overcome by immobilization of the enzymes on solid surfaces [4]. The choice of a suitable immobilization method determines parameters such as overall catalytic activity, deactivation, regeneration kinetics, and thus, the cost of process [5]. In particular, the enzyme should be immobilized in a manner that its redox center being as close as possible to the electrode base allowing rapid electron transfer with the electrode, thus, resulting in higher electrocatalytic activity of the modified electrode [6,7].

Various methods have been developed to immobilize biological compounds on the solid surfaces [8–10], however, the self-assembled monolayers (SAMs) can potentially provide a stable and robust method of constructing immobilized enzyme layers, where control over the orientation of the enzyme is offered [11].

Enzymes can be immobilized onto SAMs via electrostatic interactions [12,13], cross-linking [14], and covalent binding [15,16]. Among the different methods developed for immobilization of enzymes, direct covalent attachment onto SAMs [17,18] has been used for commercial purposes due to the high stability and possible control over surface architecture in molecular scale.

The immobilized enzymes are used for indirect [11] or direct [17,19] electron-transfer kinetic studies. In particular, direct electron transfer between the electrode surface and cofactor of the multicopper-oxidase enzymes has been a subject of interest, however, it has been studied for only a limited number of these enzymes [20–25]. Such studies can provide attractive information for the development of biocompatible and efficient electrodes in biofuel cells technology [26–28]. In addition, the design and construction of modified electrodes based on *direct electron transfer* between enzyme and the conducting support of the electrode *will eliminate the required chemical mediators and oxygen*, and thus, has a great significance in preparing the *third-generation biosensors* [20,29].

Laccase (E.C.1.10.3.2) is one of the multicopper-oxidase enzymes [20,30,31]. This enzyme can be used for several industrial, biotechnological, and biocatalytic applications. For example, applications in enzymatic oxidation of phenolic compounds [32], oxygen cathode in biofuel cells [31,33], biosensors [21], biobleaching have been reported. Laccase enzymes catalyze oxidation of several polyphenols and catecholamines with concomitant reduction of oxygen. One electron from the substrate is transferred to the T_1 site, as the primary electron acceptor of the enzyme, which is then transferred through an intermolecular electron-transfer mechanism to the T_2/T_3 cluster, where oxygen is reduced to water [20,30]. Still, one may remove oxygen, eliminate any mediator [34], and study the direct electron transfer from dopamine (DA) to enzyme, and then, from enzyme to

* Corresponding author. Tel.: +98 311 7932715.
E-mail address: rkarimi@sci.ui.ac.ir (R.K. Shervedani).

1567-5394/$ – see front matter © 2011 Elsevier B.V. All rights reserved.
doi:10.1016/j.bioelechem.2011.10.004

the conductive base of electrode [35]. Up to our knowledge, this subject has not been studied in conjunction with laccase enzymes immobilized on Au-SAMs yet.

The laccase enzymes extracted from different sources have shown different biochemical properties, depending on the source [23]. For example, laccase enzymes have formal potentials of the T_1 site ranging from +470 to +710 mV vs. NHE [24], and hence, demonstrate different catalytic performance. Accordingly, some of the laccase enzymes extracted from different sources have been immobilized on the solid supports and studied for different purposes. Examples include immobilization of laccase from: (i) Trametes versicolor on glassy carbon (GC) electrode modified by using dendrimers [34] and multi-walled carbon nanotube [36], (ii) Trametes hirsute on GC electrode [37], and (iii) Rhus Vernicifera on gold modified by cystamine [38] or 3-mercaptopropionic acid [39]. However, according to our review of the literature, there is no previous report regarding immobilization and electrochemical characterization of laccase from *Agaricus bisporus* (*LacAB*) on solid surfaces.

Dopamine (DA), one of the most important catecholamines, plays an important role in the function of the central nervous and cardiovascular system, which is a symptom of several diseases such as Schizophrenia, Parkinsonism and HIV infection. Hence, simple, rapid and reliable determination of DA in pharmaceutical injections and biological fluids with relatively low cost instrument is strongly required. Among the several methods developed for this purpose, electrochemical methods, based on enzyme modified electrodes seem to be highly promising [40,41].

The present work is intended to trace the electrochemical behavior of *LacAB*, a fungal laccase enzyme [42] immobilized on the gold-mercaptopropionic acid (Au-MPA-*LacAB* SAM) electrode, by using several electrochemical methods like cyclic and differential pulse voltammetry (CV and DPV), and electrochemical impedance spectroscopy (EIS) [43–46]. Then, the characterized electrode is used as a mediator free biosensor for detection of DA [35]. Finally, the biosensor is tested for quantitative detection of DA in pharmaceutical injection and in human blood plasma real samples. The results are presented and discussed from which the merits of the sensor are quantitatively explained.

2. Experimental

2.1. Material and reagents

Laccase (EC.1.10.3.2, from *A. bisporus*, 4 u mg^{-1}), 3-mercaptopropionic acid (MPA), 1-ethyl-3-(3-dimethylaminopropyl) carbodiimide hydrochloride (EDC), N-hydroxysuccinimide (NHS), and other chemicals were bought from commercial sources (Sigma® or Merck®). Phosphate buffer solutions (PBS) in the pH range of 5.5 to 8.5 were prepared by mixing 0.1 M KH_2PO_4/0.1 M K_2HPO_4, and acetate buffer solutions (ABS) in the pH range of 4.0 to 5.0 by 0.1 M acetic acid/0.1 M sodium acetate. The pH of the buffers was adjusted by corresponding acids or 0.1 M NaOH solutions. All solutions were prepared with deionized water (18 MΩ cm^{-1}, Millipore-MilliQ® Millipore Inc, France). Stock solutions of *LacAB* (0.3 mg ml^{-1}) were prepared in 0.1 M PBS, pH 6.5, stored at 4 °C, and allowed to equilibrate to 25 °C prior to be used in experiments. The test solutions were deaerated with high purity argon gas for 30 min before each experiment, and blanketed with the gas during the experiments. A polycrystalline gold disk electrode (Au, 99.99%, Azar electrode Co., Urmia, I.R. Iran) was used for assembly process of the enzymatic electrode. A DOPADIC® ampoule (Iran Pharmaceutical Development Investment Co., I.P.D.I.C., Rasht, I.R. Iran) containing 5 ml of 10 mmol L^{-1} DA hydrochloride was used as DA source of pharmaceutical sample. Blood plasma samples were collected from volunteers in Dr. Naser Ekramian's Medical Diagnostic Lab (Isfahan, Najafabad, I.R. Iran).

2.2. Preparation of the Au-MPA-LacAB SAM electrode

For immobilization of enzymes through SAMs, either in mediated or in direct electron transfer, a short alkyl chain alkane-thiol, usually three carbons long, is used so that the redox center of the grafted enzyme being as close as possible to the electrode [6]. Another advantage of this choice is that a relatively disordered SAM is formed which means the underlying metal is still electrochemically accessible [47]. In this study, MPA was selected as a short alkyl chain and grafted to the Au electrode (Au-MPA), and then, used as a platform to immobilize *LacAB* and fabricate Au-MPA-*LacAB* enzymatic electrode. Thus, the amine groups of the *LacAB* were coupled to the acidic head groups of Au-MPA using EDC and NHS by formation of amide group, according to the method reported in our previous works [11,48].

The gold disk electrode (surface area 0.0314 cm^2) was polished using aqueous slurries of alumina (0.30 down to 0.05 μm) and then washed ultrasonically in water/chloroform/water for 5 min to remove the physically adsorbed particles. Then, the electrode was cleaned electrochemically by cycling the electrode potential between 0.00 and +1.500 V terminated at 0.00 V vs. Ag/AgCl in 0.5 M sulfuric acid (~15 cycles, 100 mV s^{-1}), until reproducible voltammograms were observed [49]. The cyclic voltammograms obtained on the electrode in the presence of reversible marker, $K_3[Fe(CN)_6]$, showed a peak separation ($\Delta E_p \cong 77$ mV) that supported cleanness of the electrode, safety of the instrument, and properly configured cell. After rinsing with distilled water, the precleaned gold electrode was modified by sonicating in a 20 mM MPA aqueous solution for 10 min, and then, keeping in this solution for 20 h more to form Au-MPA SAM electrode. The modified electrode was washed with distilled water and then activated in 0.1 M PBS, pH 5.5, containing 0.002 M EDC and 0.005 M NHS for ~1.5 h. The activated electrode was coated with 200 μl of a 0.3 mg ml^{-1} *LacAB* solution (prepared in PBS 0.1 M, pH 6.5). The electrode coated by enzyme solution was maintained at room temperature for one hour to form Au-MPA-*LacAB* SAM enzymatic electrode. The electrode was removed, washed with the PBS, and used for electrochemical measurements.

2.3. Electrochemical measurements

Electrochemical measurements were performed in a 10 ml electrochemical cell. The CV, DPV, and EIS measurements were controlled by Potentiostat/Galvanostat Autolab 30. The modified gold disk electrode was used as working electrode, a large area Pt plate (99.99%, 5 cm^2) and a Ag/AgCl (3 M KCl) electrode were used as counter and reference electrodes, respectively. All measurements were carried out under room temperature. The modification steps were traced by CV and EIS. For the EIS studies, a 5 mV ac amplitude potential superimposed on the formal potential of the redox probe was applied, and a wide frequency range, from 10 kHz to 100 mHz, was scanned. All experiments were performed at room temperature under deareation conditions. The EIS data were approximated using ZView2.3f® software considering the fit criteria [43–45] and using appropriate equivalent circuits built in this software, from which electron-transfer kinetics as charge transfer resistance (R_{ct}), double layer capacitance (C_{dl}) and solution resistance (R_s) were extracted [50].

3. Results and discussion

3.1. Characterization of Au-MPA-LacAB

3.1.1. Electrochemical behavior of Au-MPA-LacAB electrode

The cyclic voltammograms obtained on bare Au (curve (a)), Au-MPA SAM (curve (b)) and Au-MPA-*LacAB* SAM (curve (c)) electrodes in 0.1 M PBS, pH 7, are presented in Fig. 1 (note that there was no redox probe in the solution). No faradic current was observed on the

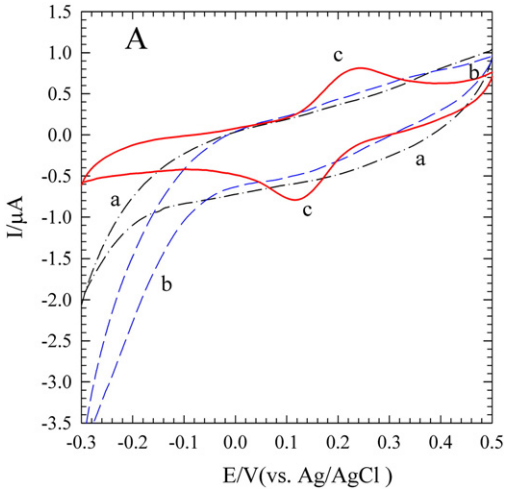

Fig. 1. Cyclic voltammograms obtained on bare Au (curve a), Au-MPA SAM (curve b) and Au- MPA-*LacAB* SAM (curve c) electrodes in PBS, pH 7. Scan rate, 100 mV s^{-1}.

bare Au and Au-MPA SAM electrodes. However, after immobilization of *LacAB*, a single well-defined redox wave with a formal potential of +180 mV vs. Ag/AgCl was observed on Au-MPA-*LacAB* SAM (curve (c)). This value, corresponding to +380 mV vs. NHE, is consistent with the T_1 copper reduction potential [51]. Only one redox couple was observed for the active *LacAB* throughout the voltammetric experiments. The separation between the anodic and cathodic peak potentials [$\Delta E_p = (E_{pa} - E_{pc}) \cong 95$ mV at 100 mV s^{-1}], and the ratio of the anodic to cathodic peak currents ($I_{pa}/I_{pc} \cong 0.81$) indicated almost a quasi-reversible cyclic voltammetric behavior for Au-MPA-*LacAB* electrode [52]. Also, the EIS complex plane plots obtained during layer-by-layer modification of the gold electrode show almost a pure capacitive effect for Au and Au-MPA, however, when the *LacAB* molecules are chemisorbed on the Au-MPA electrode, a faradaic behavior is observed (i.e. the semicircle complex plane plot start to be appeared). The faradaic behavior is attributed to the direct electron transfer between the immobilized *LacAB* molecules and the electrode base [53] (see Supplementary Information, Fig. S1). Further investigation

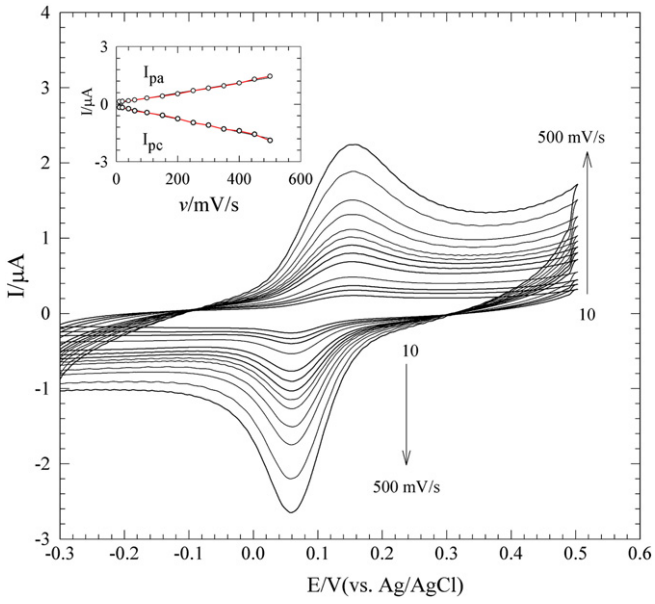

Fig. 2. Cyclic voltammograms of Au-MPA-*LacAB* SAM electrode in PBS, pH 7, scan rates from inner to outer: 10, 20, 40, 60, 80, 100, 150, 200, 250, 300, 350, 400, 450 and 500 mV s^{-1}. The inset shows variations of I_{ps} vs. scan rate.

indicated that the electron-transfer process was a surface-controlled process. The cyclic voltammograms obtained on Au-MPA-*LacAB* SAM in PBS at various sweep rates are presented in Fig. 2. The peak currents increased linearly with increasing the sweep rate (ν) in the range of 10 to 500 mV s^{-1}. This behavior demonstrates a surface confined faradaic reaction (*direct electron transfer*) for *LacAB* enzyme. We have to emphasize that the observed behavior (Fig. 2) is highly reproducible, and thus, *LacAB* immobilized on Au-MPA electrode is especially stable. Effects of the working solution pH on direct electron transfer of laccase enzymes is an important parameter [54], and thus, will be studied here.

Electrochemical behavior of Au-MPA-*LacAB* SAM electrode in various pH, from 4.0 to 8.0, was studied by CV in the *absence* of any substrate (See Supplementary Information, Fig. S2, for clarity, only few of the curves have been shown). The results indicated that an increase in the solution pH was led to an increase in the peak current up to pH ~7, then after, the currents started to decrease. Therefore, pH ~7 can be considered as the optimized pH for *LacAB* activity. Also, both reduction and oxidation peak potentials (i.e. Cu^{2+}/Cu^{+} redox reaction of Au-MPA-*LacAB*) were shifted negatively by increasing the pH, which is a normal behavior [20, 55].

3.1.2. Effect of sonication on immobilization efficiency

The voltammetric response of the Au-MPA-*LacAB* electrode towards DA oxidation was studied by DPV in two cases to verify effect of *sonication*: (i) in *presence* of DA (Fig. 3), and (ii) in the *presence* of DA and ascorbic acid (AA) or DA and uric acid (UA) (See Supplementary Information, Fig. S3).

(i) The voltammograms obtained in the absence of DA on Au-MPA-*LacAB* electrode (fabricated *without* sonication of Au-MPA) (curve a) show only one peak (peak I) which is attributed to the redox reaction of enzyme. However, the voltammograms obtained in the presence of DA on this electrode (curve b) show two peaks in which the first one (peak I that its intensity is partially increased) is independent of number of voltammogram scans while the second one (peak II) is dependent on it, i.e. its intensity is decreased by number of voltammogram scans. Peak II is attributed to the oxidation of DA at pinholes. To verify this mater, the Au was sonicated during assembly of MPA for an optimized time, 10 min.
The voltammogram obtained in the presence of DA on Au-MPA-*LacAB* electrode (fabricated *with* sonication of Au-MPA) (curve c) show only one peak that its intensity is increased by a factor of more than 3.5, and is attributed to the redox reaction of DA catalyzed by immobilized enzyme. One point should be explained here, why the intensity of peak I (curve b) is just a little increased (while more than this may be expect)? This behavior is explained in the following.
The Au-MPA fabricated *without* sonication of Au contains some pinholes, i.e. a dense MPA layer is not formed and the Au is not completely covered. Since these MPA molecules act as platform for enzyme, thus, little enzyme had been loaded on Au. This effect can cause the intensity of catalytic oxidation peak of DA (peak I, curve b) to be partially increased.
However, the reason for a large increase in the intensity of the peak I (curve c) and elimination of peak II (curve b) on the electrode fabricated *with* sonication of MPA is the assembling of a dense layer of MPA, which in turn is due to the covering of pinholes that allows loading much more enzyme on the electrode surface. The EIS complex plane plots obtained at $E_{1/2}$ (Fig. 3B) support the DPV observations. For example, the small R_{ct} obtained on Au-MPA-*LacAB* electrode is corresponded to the large faradaic current observed by DPV in these conditions (R_1 and R_2 of the inset equivalent circuit are considered as R_s and R_{ct}, respectively).

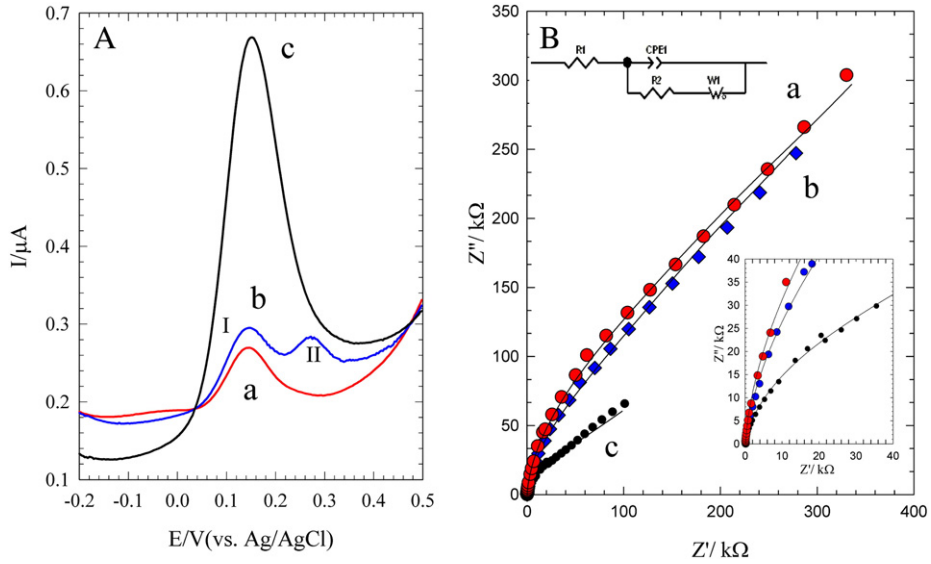

Fig. 3. (A) Differential pulse voltammograms obtained on the Au-MPA-*LacAB* SAM electrode fabricated: *Without* sonication of Au-MPA; (curve a) in the absence of DA and (curve b) in the presence of DA. And *with* sonication of Au-MPA; (curve c) in the presence of DA. The DA concentration was 4 μmol L^{-1} DA, when it was present in the test solution. (B) The EIS complex plane plots obtained at $E_{1/2}$ in the frequency range of 10 kHz to 100 mHz, in the same conditions as (A).

(ii) The voltammograms obtained on Au-MPA-*LacAB* electrode (See Supplementary Information, Fig. S3) in the presence of DA (curve a) and AA (curve b) on Au-MPA-*LacAB* electrode (fabricated *without* sonication of Au-MPA) show that AA is oxidized together with DA at pinholes (peak II, curve b). However, on the electrode fabricated *with* sonication, this peak (peak II) is not observed (Fig. S3, curve c). Similar behavior was observed when UA was used instead of AA. This behavior supports several points; selective response of this enzyme electrode to DA (see also Section 3.2.2.2), effect of sonication on formation of a dense layer of MPA, and thus, immobilization efficiency assisted by application of the ultrasounds.

3.2. Analytical characteristics of Au-MPA-LacAB SAM as a biosensor towards DA

3.2.1. Electrocatalytic behavior of Au-MPA-LacAB electrode towards DA

The electrocatalytic behavior of Au-MPA-*LacAB* electrode towards the DA was studied to find the possible application of Au-MPA-*LacAB* SAM electrode for quantitative detection of DA, first. Then, the method was calibrated and its application for determination of DA in real samples was tested.

Electrocatalytic activity of Au-MPA-*LacAB* SAM electrode towards the DA was evaluated by DPV. The voltammograms obtained on (a) bare Au, (b) Au-MPA SAM, and (c) Au-MPA-*LacAB* SAM electrodes in the presence of DA are displayed in Fig. 4A. The oxidation potential of DA (~+220 mV) on bare Au was shifted to more anodic potentials (~+360 mV) on Au-MPA SAM. This shift could be mostly due to isolation effect of MPA. However, on Au-MPA-*LacAB* SAM electrode, the potential was shifted to negative (more facile) direction (~+170 mV) and the related peak current increased by a factor of ~10 (compare curves (b) and (c)), which is due to oxidation of DA in oxidation potential range of immobilized LacAB, so called *direct electrocatalysis* of DA by LacAB. An increase in current or a shift in reaction potential to more facile direction for an electrochemical reaction observed on a modified electrode surface is called *electrocatalytic effect* of the modifier. Interestingly, here, both effects are observed for *LacAB* toward the DA. The EIS complex

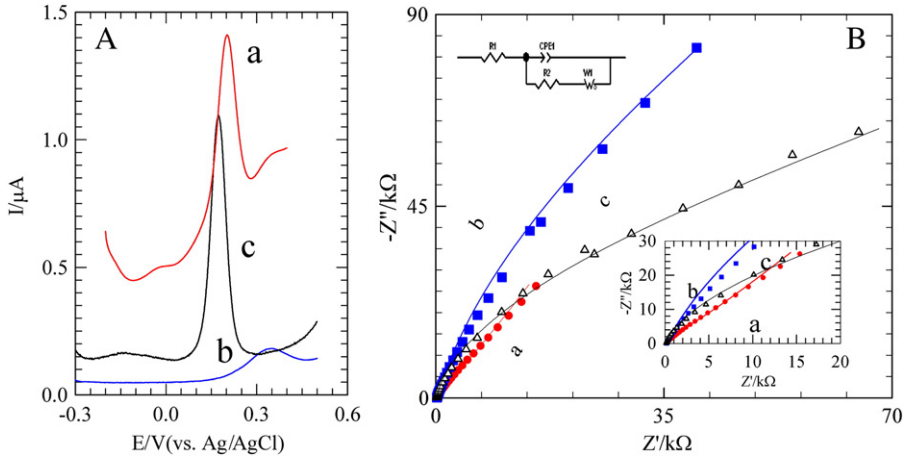

Fig. 4. (A) Differential pulse voltammograms obtained on (a) bare Au, (b) Au-MPA SAM and (c) Au-MPA-*LacAB* SAM electrodes in 0.1 M PBS, pH 7, in the presence of 0.02 mmol L^{-1} DA in solution. The DPV conditions were as: interval time: 400 ms; modulation time: 10 ms; step potential: 30 mV; modulation amplitude: 40 mV. (B) The EIS complex plane plots obtained at $E_{1/2}$ in the frequency range of 10 kHz to 100 mHz, in the same conditions as (A). The inset of (B) shows equivalent circuit used for approximation of the EIS data, in which R_1 and R_2 are considered as R_s, and R_{ct} respectively.

plane plots obtained in the same condition at $E_{1/2}$ (Fig. 4B) support the DPV observations (note that $1/R_{ct}$ behaves similar to the faradaic current).

We should emphasize that oxygen has been removed from the solution, and the experiments have been performed under pure argon atmosphere to eliminate effect of oxygen mediation and perform the electrooxidation of DA under direct electron transfer. Thus, this study indicates the direct electron transfer from DA (as substrate) to enzyme, and then, from enzyme to the conductive base of the electrode. Up to our knowledge, this subject is reporting in conjunction with laccase enzymes immobilized on Au-SAMs for the first time here. The proposed mechanism is given in Supplementary Information, after Fig. S3.

The abovementioned examination revealed that Au-MPA-*LacAB* SAM electrode was an efficient *electrocatalyst* for detection of DA at the ambient temperature and the operational instrumental conditions. More experiments were performed to investigate the electrocatalytic activity of the Au-MPA-*LacAB* SAM biosensor in the *presence* of DA in various pH, from 4 to pH 8. Variations of the voltammetric oxidation peak current of 0.02 mM DA vs. pH showed that the maximum activity was obtained between pH 6 to 7 (Fig. 5, for clarity only some of the curves are presented).

The probable reason for this behavior is explained as follows: At pHs higher than 7, the OH^- binds to T_2/T_3 sites of laccase and inhibits the enzyme–substrate interaction, resulting in a decrease in biological activity of enzyme [54,56]. At pHs lower than 6, the amine groups, of both DA [40] and enzyme, are partially positively charged, and thus, the activity decreases due to electrostatic interactions (repulsion). Besides; denaturation of the enzyme at 7<pH<6 and the effect of pH on redox reaction of DA are significant and should be considered. The observed activity is a resultant of all these effects. Thus, the pH 7.0 that was very close to the physiological pH, was selected for the electrochemical detection of DA.

Finally; the oxidation potential (E_{pa}) of DA is shifted linearly to negative direction by increasing the solution pH with a slope of 58 mV/pH (r = 0.996) in the range of 4.0 to 8.5 (Fig. 5), implying that the redox reaction of DA undergoes a 1:1 for e^-:H^+ process.

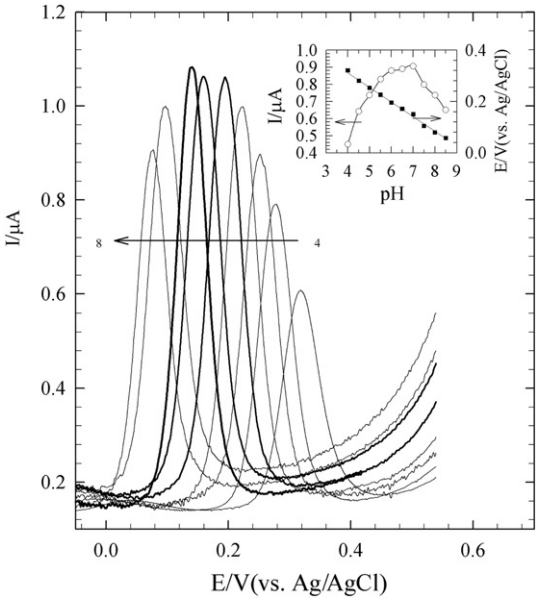

Fig. 5. Voltammetric response of Au-MPA-*LacAB* SAM electrode in a 0.02 mmol L^{-1} DA solution as a function of pH, buffered from 4.0 to 8.5. For clarity, only some of the curves are presented. Insets show variations of the oxidation potential and current as a function of solution pH.

3.2.2. Calibration and analytical application

3.2.2.1. Calibration and detection limit. Quantitative response of Au-MPA-*LacAB* to DA was studied in 0.1 M PBS, pH 7, by gradual addition of DA and recording the related differential voltammograms. Typical voltammograms obtained on Au-MPA-*LacAB* SAM electrode as a function of DA concentration are presented in Fig. 6A. A wide linear range with two parts, from 0.5 to 13 μmol L^{-1} and 47.0 to 430.0 μmol L^{-1} DA as we have shown by Eqs. (1) and (2), respectively, and a detection limit of 29.0 nmol L^{-1} DA estimated using 3δ as signal, where δ was standard deviation for (n = 5) measurements in blank reagent solution (Fig. 6B).

$$\left[I_p/\mu A = (6.12 \pm 0.10) \times 10^{-2}[DA]/\mu M - (1.35 \pm 0.20) \times 10^{-8}/\mu A\right] \quad (1)$$

$$\left[I_p/\mu A = (2.29 \pm 0.10) \times 10^{-2}[DA]/\mu M + (78.00 \pm 0.60) \times 10^{-8}/\mu A\right] \quad (2)$$

A comparison between the detection limit obtained in this work (29.0 nmol L^{-1} DA) with that recently published (448 nmol L^{-1} DA) using a similar enzymatic biosensor electrode based on "bean sprout peroxidase" [40], indicates that the detection limit and the linear range of this work are ~17 times lower and more than one order of magnitude larger, respectively.

3.2.2.2. Interferences. To evaluate the selectivity of the Au-MPA-*LacAB* SAM electrode, the influence of some possible interference substances were investigated in the presence of DA. Interfering effect is defined as the concentration of interfering species that can change the electrode response toward the analyte by more than 3δ, where δ is standard deviation of the replicate. The criterion used for the presence of interference was the *t*-test at 95% confidence level. The results showed that a 25-fold excess of UA and 14-fold excess of AA did not interfere in the determination of DA (see Supplementary Information, Fig. S4). Also, the Au-MPA-*LacAB* electrode was tested in the absence of DA for either AA or UA in the same conditions. The results revealed no significant signal for these cases (see Supplementary Information, Figs. S5 and S6). High selectivity of Au-MPA-*LacAB* is due to (i) selective nature and electrocatalytic effect of the enzyme based biosensor (E_{pa} and I_{pa} on Au-MPA-*LacAB* were ~200 mV and 10 times better than those observed on Au-MPA) and (ii) antifouling effect of SAM.

3.2.2.3. Stability, repeatability, and reproducibility. The *stability* of Au-MPA-*LacAB* electrode was investigated by recording the electrode response in 0.1 M PBS pH 7 containing 50 μM DA, once in every day. There were no significant changes in the electrode response, where the electrode was kept in 0.1 M PBS, pH 7, during the measurements for one week. The relative standard deviation of the peak currents for 7 times measurements, and each time (n = 5) was found to vary from 2.7% to 3.5%. *The repeatability* of the electrode response was estimated by making repetitive determinations of 50 μmol L^{-1} DA using one Au-MPA-*LacAB* electrode. The relative standard deviation of the peak currents for (n = 5) was found to be 3.2%. *The reproducibility* of the electrode response was examined by fabrication of a set of four Au-MPA-*LacAB* electrodes, and then, recording the electrode response in 0.1 M PBS, pH 7, containing 50 μmol L^{-1} DA. The relative standard deviation of the peak currents for (n = 4) was found to be 3.2%. These examinations indicated high stability, repeatability, and reproducibility of the electrode response to DA.

3.2.2.4. Analysis of the real samples. Blood plasma and pharmaceutical injection samples were used as models of real samples to evaluate practical utility of the proposed biosensor, Au-MPA-*LacAB*. Two milliliters

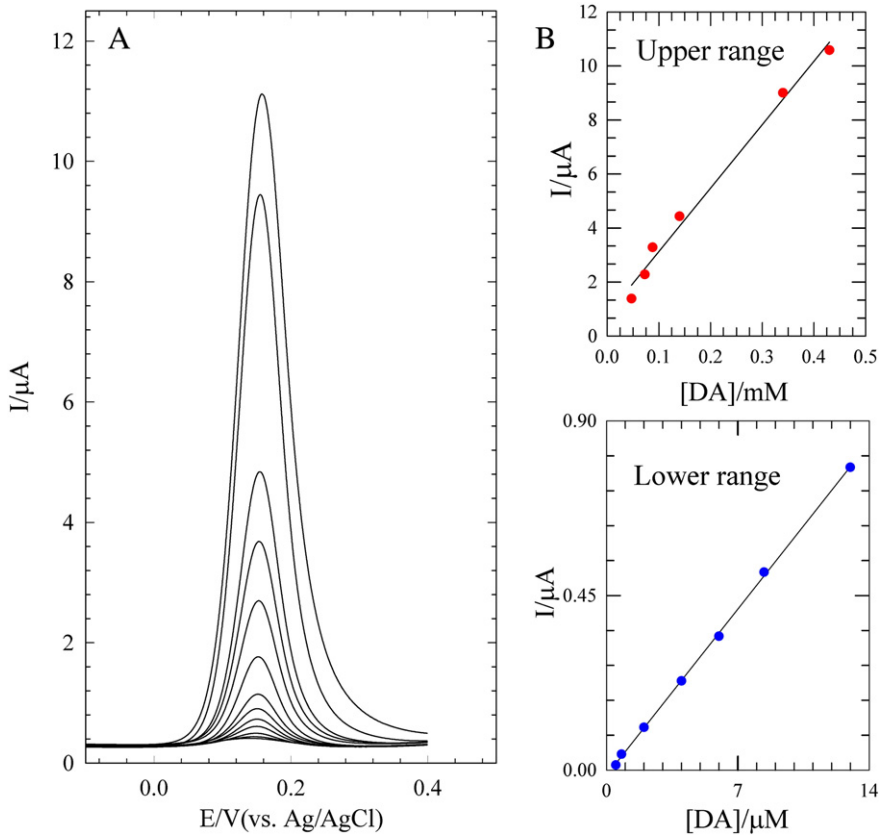

Fig. 6. (A) Differential pulse voltammograms of DA at the Au-MPA-*LacAB* SAM electrode under optimum conditions. DA concentration (inner to outer) 5×10^{-7}, 8.4×10^{-7}, 2×10^{-6}, 4×10^{-6}, 6×10^{-6}, 8.7×10^{-6} and 1.3×10^{-5} mol L^{-1} DA and 4.7×10^{-5}, 7.3×10^{-5}, 8.8×10^{-5}, 1.4×10^{-4}, 3.4×10^{-4}, and 4.5×10^{-4} mol L^{-1} DA. (B) The calibration curves are also given for lower and upper ranges. The signals are corrected for background (blank) currents.

of 0.125 M sodium citrate, was added to 18 mL of fresh blood sample (collected from volunteers, see Section 2.1) and mixed. Then, the solution was centrifuged at the revolution rate of 3000 rpm. After 5 min, three phases were appeared. The above phase (plasma) was separated and used for next step. Four portions of 1.0 mL of this phase were used for quantitative analysis by electrochemical methods. The pharmaceutical samples were used without special treatment.

Both pharmaceutical and plasma samples were spiked with certain amounts of DA, the related voltammogram were recorded, and the amount of DA was determined using I_ps. The results of the recovery tests (Table 1) showed that the proposed methods could be efficiently used for the determination of DA in pharmaceutical and human blood plasma samples.

Table 1
Results of the recovery tests obtained for determination of DA in pharmaceutical injection and human blood plasma samples.

Sample	DA[a] added (μM)	DA obtained[a] (μM)	Recovery%
Pharmaceutical injection sample	0.00	5.06	101.0
	6.00	10.90	99.3
	16.00	20.60	97.9
Human blood plasma[b]	0.50	0.52	104.0
	5.50	5.62	102.0
	15.50	15.34	98.9

[a] The results are average of three measurements.
[b] Concentration of DA in blood plasma obtained from "normal people" was lower than the detection limit of the method. We hoped to find patients suffer from diseases like Alzheimer, Schizophrenia, or Parkinsonism to test our method for determination of DA in their blood plasma. However, we could not find any case during the course of this project.

4. Conclusions

In this study, a new laccase enzyme was successfully immobilized on gold via 3-mercaptopropionic acid, and its direct electron-transfer behavior was studied by using CV, DPV, and EIS techniques. The characterized electrode was used as a third generation biosensor for determination of dopamine (DA). Excellent results were obtained by using the sensor fabricated based on MPA assembled *with* sonication. Other optimized conditions for biosensor response to DA were 0.1 M PBS, pH 7 at ambient temperature according to DPV and EIS results. The studies of the interferences showed that a 25-fold excess of UA and 14-fold excess of AA did not interfere significantly in the determination of DA at 95% confidence level. The described biosensor was successfully tested for determination of DA in pharmaceutical injection as well as in human blood plasma real samples. The sensor showed good stability, for one test a day in a period of one week.

Acknowledgements

The authors gratefully acknowledge the University of Isfahan for providing research facilities. Special thanks to Dr. Naser Ekramian's Medical Diagnostic Lab (Isfahan, Najafabad, I.R. IRAN) for sharing his Lab facilities, collection of blood samples, and preparation of blood plasma. Also, thanks to Mr. Hosein Ali-Najafi Najafabadi for his help in collection of volunteers' blood samples and preparation of the related plasma.

Appendix A. Supplementary data

Supplementary data to this article can be found online at doi:10.1016/j.bioelechem.2011.10.004.

References

[1] M. Alcalde, M. Ferrer, Francisco J. Plou, A. Ballesteros, Environmental biocatalysis: from remediation with enzymes to novel green processes, Biotechnology 24 (2006) 281–287.
[2] L.J. Blum, P.R. Coulet, in: J. Cooper, T. Cass (Eds.), Biosensors, 2nd ed., Oxford University Press, New York, 2004.
[3] I. Roy, S. Sharma, M.N. Gupta, in: T. Scheper (Ed.), New Trends and Developments in Biochemical Engineering, vol. 86, Springer, Berlin, 2004.
[4] N. Vasileva, T. Godjevargova, Study of effect of some organic solvents on the activity and stability of glucose oxidase, Mater. Sci. Eng., C 25 (2005) 17–21.
[5] M.Y. Arica, Immobilization of polyphenol oxidase on carboxymethylcellulose hydrogels beads: preparation and characterization, Polym. Int. 49 (2000) 775–781.
[6] M. Mrksich, G.M. Whitesides, Using self-assembled monolayers to understand the interactions of man-made surfaces with proteins and cells, Annu. Rev. Biophys. Biomol. Struct. 25 (1996) 55–78.
[7] J.J. Gooding, D.B. Hibbert, The application of alkanethiol self-assembled monolayers to enzyme electrodes, Trends Anal. Chem. 18 (1999) 525–533.
[8] A.I. Yaropolov, A.N. Kharybin, J. Ermneus, G.M. Varga, L. Gorton, Electrochemical properties of some copper-containing oxidases, Bioelectrochem. Bioenerg. 40 (1996) 49–57.
[9] M. Gerard, A. Chanbey, B.D. Malhota, Application of conducting polymers to biosensors, Biosens. Bioelectron. 17 (2002) 435–439.
[10] N.K. Chaki, K. Vijayamohanan, Self-assembled monolayers as a tunable platform for biosensor applications, Biosens. Bioelectron. 17 (2002) 1–12.
[11] R.K. Shervedani, Z. Hemmatian, A. Hatefi-Mehrjardi, Immobilization of L-lysine α-oxidase on gold-mercaptopropionic acid self-assembled monolayer: preparation and electrochemical characterization, Bioelectrochemistry 75 (2009) 124–129 and references therein.
[12] J. Li, J. Yan, Q. Deng, G. Cheng, S. Dong, Viologen-thiol self-assembled monolayers for immobilized horseradish peroxidase at gold electrode surface, Electrochim. Acta 42 (1997) 961–967.
[13] J. Hodak, R. Etchenique, E.J. Calvo, K. Singhal, P.N. Bartlett, Layer-by-layer self-assembly of glucose oxidase with a poly(allylamine)ferrocene redox mediator, Langmuir 13 (1997) 2708–2716.
[14] M. Imamura, T. Haruyama, E. Kobatake, Y. Ikariyama, M. Aizawa, Self-assembly of mediator-modified enzyme in porous gold-black electrode for biosensing, Sens. Actuators, B 24 (1995) 113–116.
[15] J. Li, G. Cheng, S. Dong, Direct electron transfer to cytochrome c oxidase in self-assembled monolayers on gold electrodes, J. Electroanal. Chem. 416 (1996) 97–104.
[16] J.J. Gooding, V. Praig, E.A.H. Hall, Platinum-catalyzed enzyme electrodes immobilized on gold using self-assembled layers, Anal. Chem. 70 (1998) 2396–2402.
[17] T. Loëtzbeyer, W. Schuhmann, H.L. Schmidt, Electron transfer principles in amperometric biosensors: direct electron transfer between enzymes and electrode surface, Sens. Actuators, B 33 (1996) 50–54.
[18] E. Katz, I. Willner, Probing biomolecular interactions at conductive and semiconductive surfaces by impedance spectroscopy: routes to impedimetric immunosensors, DNA-sensors, and enzyme biosensors, Electroanalysis 15 (2003) 913–947.
[19] J. Wang, Glucose biosensors: 40 years of advances and challenges, Electroanalysis 13 (2001) 983–988.
[20] E.I. Solomon, U.M. Sundaram, T.E. Machonkin, Multicopper oxidases and oxygenases, Chem. Rev. 96 (1996) 2563–2605.
[21] S.R. Couto, J.L.T. Herrera, Industrial and biotechnological applications of laccases, a review, Biotechnol. Adv. 24 (2006) 500–513.
[22] K. Haberska, C. Vaz-Domínguez, A.L. DeLacey, M. Dagys, C.T. Reimann, S. Shleev, Direct electron transfer reactions between human ceruloplasmin and electrodes, Bioelectrochemistry 76 (2009) 34–41.
[23] S. Shleev, J. Tkac, A. Christenson, T. Ruzgas, A.I. Yaropolov, J.W. Whittaker, L. Gorton, Direct electron transfer between copper-containing proteins and electrodes, Biosens. Bioelectron. 20 (2005) 2517–2554.
[24] S. Shleev, A.J. Wilkolazka, A. Khalunina, O. Morozova, A. Yaropolov, T. Ruzgas, L. Gorton, Direct electron transfer reactions of laccases from different origins on carbon electrodes, Bioelectrochemistry 67 (2005) 115–124.
[25] P. Ramirez, N. Mano, R. Andreu, T. Ruzgas, A. Heller, L. Gorton, S. Shleev, Direct electron transfer from graphite and functionalized gold electrodes to T1 and T2/T3 copper centers of bilirubin oxidase, Biochim. Biophys. Acta 1777 (2008) 1364–1369.
[26] S.C. Barton, J. Gallaway, P. Atanassov, Enzymatic biofuel cells for implantable and microscale devices, Chem. Rev. 104 (2004) 4867–4886.
[27] A. Heller, Miniature biofuel cells, Phys. Chem. Chem. Phys. 6 (2004) 209–216.
[28] D. Ivnitski, P. Atanassov, Electrochemical studies of intramolecular electron transfer in laccase from Terametes versicolor, Electroanalysis 19 (2007) 2307–2313.
[29] J.J. Gooding, E.A.H. Hall, D.B. Hibbert, From thick films to monolayer recognition layers in amperometric enzyme electrodes, Electroanalysis 10 (1998) 1130–1136.
[30] O.V. Morozova, G.P. Shumakovich, M.A. Gorbacheva, S.V. Shleev, A.I. Yaropolov, "Blue" laccases, J. Biochem. 72 (2007) 1136–1150.
[31] G. Gupta, V. Rajendran, P. Atanassaov, Laccase biosensor on monolayer-modified gold electrode, Electroanalysis 15 (2003) 1577–1583.
[32] G. Bayramoğlu, M.Y. Arıca, Immobilization of laccase onto poly(glycidylmethacrylate) brush grafted poly(hydroxyethylmethacrylate) films: enzymatic oxidation of phenolic compounds, Mater. Sci. Eng., C 29 (2009) 1990–1997.
[33] G.T.R. Palmore, H.H. Kim, Electro-enzymatic reduction of dioxygen to water in the cathode compartment of a biofuel cell, J. Electroanal. Chem. 464 (1999) 110–117.
[34] M.R. Aminur, N.B. Hui, Y.B. Shim, Direct electrochemistry of laccase immobilized on Au nanoparticles encapsulated-dendrimer bonded conducting polymer: application for a catechin sensor, Anal. Chem. 80 (2008) 8020–8027.
[35] R.S. Freire, C.A. Pessoa, L.D. Mello, L.T. Kubota, Direct electron transfer: an approach for electrochemical biosensor with higher selectivity and sensitivity, J. Braz. Chem. Soc. 14 (2003) 230–243.
[36] M. Klis, E. Maicka, A. Michota, J. Bukowska, S. Sek, J. Rogalski, R. Bilewicz, Electroreduction of laccase covalently bound to organothiol monolayers on gold electrodes, Electrochim. Acta 52 (2007) 5591–5598.
[37] A. Yaropolov, S. Shleev, E. Zaitseva, J. Emneus, G. Marko-varga, L. Gorton, Electroenzymatic reactions with oxygen on laccase-modified electrodes in anhydrous (pure) organic solvent, Bioelectrochemistry 70 (2007) 199–204.
[38] G. Gupta, V. Rajendran, P. Atanassov, Bioelectrocatalysis of oxygen reduction reaction by laccase on gold electrodes, Electroanalysis 16 (2004) 1182–1185.
[39] E. Casero, M. Darder, F. Pariente, E. Lorenzo, Thiol-functionalized gold surfaces as a strategy to induce order in membrane-bound enzyme immobilization, Nano Lett. 2 (2002) 577–582.
[40] S.K. Moccelini, S.C. Fernandes, I.C. Vieira, Bean sprout peroxidase biosensor based on l-cysteine self-assembled monolayer for the determination of dopamine, Sens. Actuators, B 133 (2008) 364–369.
[41] X. Ling, L. Yuqing, S. Lei, M. Lanqun, Laccase-catalyzed oxidation and intramolecular cyclization of dopamine: a new method for selective determination of dopamine with laccase/carbon nanotube-based electrochemical biosensors, Electrochim. Acta 52 (2007) 4144–4152.
[42] S.E. Matcham, D.A. Wood, Purification of *Agaricus bisporus* extracellular laccase from mushroom compost, Biotechnol. Lett. 14 (1992) 297–300.
[43] E. Sabatani, I. Rubinstein, Organized self-assembling monolayers on electrodes. 2. Monolayer-based ultramicroelectrodes for the study of very rapid electrode kinetics, J. Phys. Chem. 91 (1987) 6663–6669.
[44] R.K. Shervedani, M. Bagherzadeh, Hydroxamation of gold surface via in-situ layer-by-layer functionalization of cysteamine self-assembled monolayer: preparation and electrochemical characterization, Electrochim. Acta 53 (2008) 6293–6303.
[45] R.K. Shervedani, A.R. Madram, Kinetics of hydrogen evolution reaction on nanocrystalline electrodeposited $Ni_{62}Fe_{35}C_3$ cathode in alkaline solution by electrochemical impedance spectroscopy, Electrochim. Acta 52 (2007) 426.
[46] R.K. Shervedani, S.A. Mozaffari, Impedimetric sensing of uranyl ion based on phosphate functionalized cysteamine self-assembled monolayers, Anal. Chim. Acta 562 (2006) 223–228.
[47] J.J. Gooding, P. Erokhin, D. Iosic, W. Yang, V. Policarpio, J. Liu, F.M. Ho, M. Situmorang, D.B. Hibbert, J.G. Shapter, Parameters important in fabricating enzyme electrodes using self-assembled monolayers of alkanethiols, Anal. Sci. 17 (2001) 3–9.
[48] R.K. Shervedani, A. Hatefi-Mehrjardi, N. Zamiri, A novel method for glucose determination based on electrochemical impedance spectroscopy using glucose oxidase self-assembled biosensor, Bioelectrochemistry 69 (2006) 201–208.
[49] J.P. Hoare, A cyclic voltammetric study of the gold–oxygen system, J. Electrochem. Soc. 131 (1984) 1808–1815.
[50] R. Jurczakowski, C. Hitz, A. Lasia, Impedance of porous gold electrodes in the presence of electroactive species, J. Electroanal. Chem. 582 (2005) 85–96.
[51] W. Zheng, L. Qingfen, S. Lei, Y. Yiming, J. Zhang, M. Lanqun, Direct electrochemistry of multi-copper oxidases at carbon nanotubes noncovalently functionalized with cellulose derivatives, Electroanalysis 18 (2006) 587–594.
[52] Y. Tian, L. Mao, T. Okajima, T. Ohsaka, Superoxide dismutase-based third-generation biosensor for superoxide anion, Anal. Chem. 74 (2002) 2428–2434.
[53] L. Wang, E. Wang, A novel hydrogen peroxide sensor based on horseradish peroxidase immobilized on colloidal Au modified ITO electrode, Electrochem. Commun. 6 (2004) 225–229.
[54] F. Xu, Effects of redox potential and hydroxide inhibition on the pH activity profile of fungal laccase, J. Biol. Chem. 272 (1997) 924–928.
[55] C. Leger, F. Lederer, B. Guigliarelli, P. Bertrand, Electron flow in multicenter enzymes: theory, applications and consequences on the natural design of redox chains, J. Am. Chem. Soc. 128 (2006) 180–187.
[56] R. Santucci, T. Ferri, L. Morpurgo, I. Savini, L. Avigliano, Unmediated heterogeneous electron transfer reaction of ascorbate oxidase and laccase at a gold electrode, J. Biochem. 332 (1998) 611–615.